EPSC Abstracts
Vol. 13, EPSC-DPS2019-119-1, 2019
EPSC-DPS Joint Meeting 2019

EPSC
EPSC-DPS Joint Meeting 2019
15–20 September 2019 | Geneva, Switzerland

Border variability of transit light-curves

Maxim L. Khodachenko (1,2,3), Oleksiy V. Arkhypov (1), Manuel Güdel (4)
(1) Space Research Institute, Austrian Academy of Science, Graz, Austria, (2) Skobeltsyn Institute of Nuclear Physics, Moscow State University, Moscow, 119992, Russia, (3) Institute of Astronomy of the Russian Academy of Sciences, 119017, Moscow, Russia, (4) Institute of Astronomy, University of Vienna, Vienna, Austria (maxim.khodachenko@oeaw.ac.at)

Abstract

A model-independent method for detection of transit borders, using the polynomial approximation of the light-curve parts, is proposed. The trial processing of long-cadence light-curves of 183 *Kepler's* exoplanets reveals for some objects a variability of transit's start/end- times and asymmetry. The diagnostic diagram was constructed for preliminary classification and interpretation of such results.

1. Introduction

Hitherto studies on variability of exoplanetary transit timing and depth supposed the symmetric shape of a transit light-curve (TLC) suggesting a spherical exoplanet (e.g., [1]). As a result, the independent positions of transit borders and minimum were not considered. However, exactly the border parts of a TLC are most sensitive to the shape of a transiting matter, e.g., to exo-rings and dust formations which are of great interest. For the first time we explore independent location of transit borders, detecting their unstudied so far variations.

2. Method

We use publically available *Kepler* long cadence light-curves [2] after Pre-search Data Conditioning. After an iterative whitening and exclusion of outliers we obtain the flux decrease ΔF during the transit, which is used in further analysis. To increase the number of measurement points in the analyzed TLC, we fold it in each of adjacent equidistant time-windows using the relative time $\Delta t = t - t_E$. Here t and $t_E = t_0 + P_{tr}E$ are the current flux count time and one, recalculated in reference fame of the transit with number E, respectively, using the transit period P_{tr} and t_0 (the mid-time of first observed transit) from [2]. Since the time-window typically covers ~25 transits, the irregular fluctuations of folded TLCs by sporadic starspots are averaged. To determine independently the relative start/end-, and minimum- times (Δt_s, Δt_e and Δt_m) of a folded TLC, we separately approximate its corresponding ingress/egress and middle parts with the second-order polynomials. Although this method could give systematic errors related with the applied approximating polynomial order and TLC-smoothing by the long-cadence exposition (0.02 day), such constant displacements are inessential for the study of transit *variability*. For the analysis of obtained estimates of Δt_s, Δt_e and Δt_m the diagnostic parameters: the Pearson correlation coefficient r_{se} between Δt_s, and Δt_e and the transit asymmetry $A_s = (\Delta t_m - \Delta t_s)/(\Delta t_e - \Delta t_s)$ are used.

3. Results

Our data set includes long-cadence TLCs of 183 Kepler's objects with maximal signal-to-noise ratio. In some cases we found transits with oscillating Δt_s or Δt_e (Fig. 1), whereas Δt_m remains quasi-constant, as well as variable A_s (Fig. 2). Such behaviour resembles the modelled effects from a precessing ring (Fig. 3).

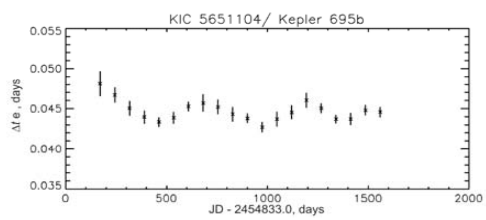

Figure 1: Example of the variable transit border Δt_e while the transit min-time Δt_m is practically constant.

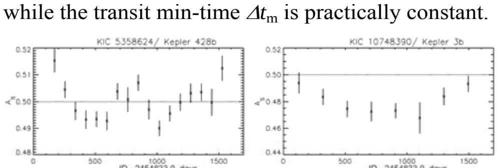

Figure 2: Examples of the variable transit asymmetry.

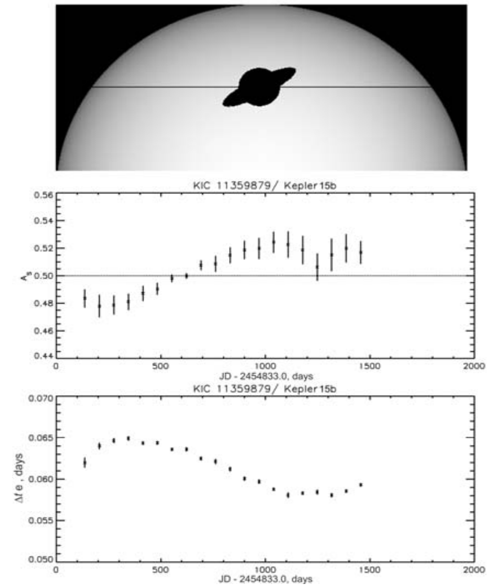

Figure 3: Modeling of transit variability for the planet Kepler-15b with an imposed precessing ring (30^{o}inclination to the orbital plane, period 2400 days).

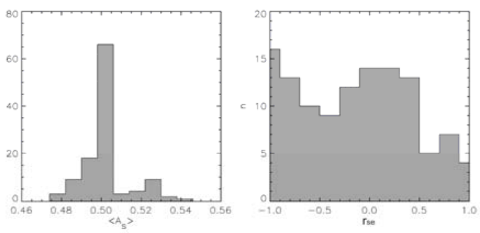

Figure 4: Distributions of 117 best estimates $<A_s>$ and r_{se} with the error of $<A_s>$ under 0.05.

According to modeling (see Fig. 3), the inclined ring, precessing with a period $>10^4$ days could result in a perceptible TLC asymmetry $|<A_s>—0.5|>0.01$ and low $|r_{se}|<0.3$ (Fig. 4). This prognosis is reflected in Fig. 5, among other possible cases, as the rose ellipse. The orange domain in Fig.5 ($r_{se}<-0.3,<A_s>\approx0.5$) corresponds to variable impact parameter (IP) or size of the transiting object. The green domain ($r_{se}>0.3,<A_s>\approx0.5$) depicts the transit shifts in time due to longitudinal perturbations. The blue domain ($<A_s>$ below ≈0.48) contains possible tail-like dust formations, whereas the late minimum relative TLC

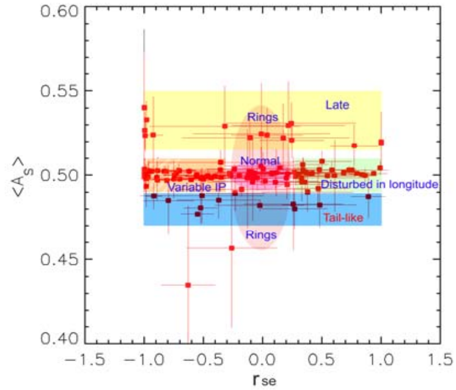

Figure 5: Diagnostic diagram for the same population (red squares) as in Fig. 4. The coloured schematic of cluster domains is labelled with interpretations.

center corresponds the yellow domain with $<A_s>$ above 0.5.

4. Summary and Conclusions

Since the starspots have sporadic and local character, they cannot produce correlation effects between the start and end times, which are significant ($|r_{se}|>0.5$) in many cases (see Figs. 4 and 5). Regular oscillations of Δt_e and A_s (Figs.1 and 2), as well as modeling in Fig. 3, argue for the reality of found TLCs' border variability. Such variability is a promising, but so far unused source of information on exo-rings, circumplanetary dust and planetary dynamics.

Acknowledgements

This work was performed as a part of the project S11606-N16 of the Austrian *Fonds zur Förderung der wissenschaftlichen Forschung*, FWF. MLK also thanks Russian Science Foundation RSF project 18-12-00080.

References

[1] Holczer, T., Mazeh, T., Nachmani, G., et al. Transit timing observations from Kepler. IX. Catalog of the full long-cadence data set, *Astrophys. J. Suppl. Ser*., **225**, 9, 2016.

[2] NASA Exoplanet Archive, https://exoplanetarchive.ipac.caltech.edu/